Title no. 103-M22

Constitutive Model for Alkali-Aggregate Reactions

by Victor Saouma and Luigi Perotti

A new constitutive model for alkali-aggregate reaction (AAR) expansion is presented. This thermo-chemo-mechanical model is rooted in the chemistry, physics, and mechanics of concrete. The major premises of the model are the assumption of a volumetric expansion of the gel and redistribution on the basis of weights related to the stress tensor (hence induced anisotropy). This three-component model is, for the most part, loosely coupled, with the exception of the interdependency between the mechanical and the chemical parts through the kinetics of the reaction. The model has been used, in conjunction with a formal parameter identification paradigm, to analyze laboratory tests on triaxially confined concrete cylinders. Finally, a detailed two-dimensional analysis of an arch gravity dam is presented.

Keywords: alkali-aggregate reaction; alkali-silica reaction; dams; model.

INTRODUCTION

Alkali-aggregate reaction (AAR), which includes alkali-silica reaction (ASR), is the leading cause of dam concrete deterioration. This slow-evolving internal concrete damage is causing millions of dollars of damage worldwide, and whereas there is no (economically) feasible method to stop the reaction, it can be mitigated to some extent. This has been accomplished primarily through an expensive slicing of the dam to relieve the reaction-induced compressive stresses. Hence, given the need to plan this complex mitigation procedure, and keeping in mind that in some drastic cases the dam may have to be decommissioned, there is an urgent need to provide the engineering profession with solid, sound, and practical predictive tools for the dam structural response evolution.

ASR in concrete is a chemical reaction involving alkali cations and hydroxyl ions from concrete pore solutions, and certain metastable or strained forms of silica present within aggregate particles. This chemical reaction will produce ASR gel that swells with the absorption of moisture. Hence, in a simplified manner, ASR can be described as a two-step reaction between alkalis (sodium and potassium) in concrete and silica reactive aggregates. The first step is the chemical reaction between the reactive silica in the aggregate with the alkali present in concrete to produce alkali-silica gel

$$\begin{gathered}\text{Reactive silica in aggregate + alkali in concrete} \rightarrow \\ \text{alkali-silica gel} \\ [x\mathrm{SiO_2}] + [y\mathrm{Na(K)OH}] \rightarrow [\mathrm{Na(K)}_y\mathrm{SixO}_z\mathrm{aq}]\end{gathered} \qquad (1)$$

The second step is the expansion of the alkali-silica gel when it comes in contact with moisture

$$\begin{gathered}\text{Alkali-silica gel + moisture} \rightarrow \text{expanded alkali-silica gel} \\ [\mathrm{Na(K)}_y\mathrm{Si}_x\mathrm{O}_z\mathrm{aq}] + [\mathrm{H_2O}] \rightarrow [\mathrm{Na(K)}_y\mathrm{Si}_x\mathrm{O}_z w\mathrm{H_2O}]\end{gathered} \qquad (2)$$

It is precisely this second reaction that causes the well-known swelling of the concrete, resulting in major internal stress redistribution inside the dam that manifests itself either through large compressive stresses, and/or more dramatically through the formation of structural cracks or the sliding across critical joints. Hence, the structural integrity of the structure can certainly be seriously jeopardized by the pernicious and slow evolution of the reaction.

RESEARCH SIGNIFICANCE

Many concrete dams worldwide are affected by AARs, and despite much research, there is still a dichotomy between models and applications. Models tend to be too narrowly defined and are seldom applied to actual structures where all the complexity of the load is accounted for.

The proposed model is comprehensive; it is rooted in the chemistry, physics, and mechanics of AAR and derives much of its parameters from recent experimental tests performed at the Laboratoire Centrale des Ponts et Chaussées (LCPC), France.

A peculiarity of AAR in dams is that there are field measurements of the irreversible crest displacement that in theory should be matched by the numerical model. So far, this has been an ad-hoc process through "manual" fine-tuning. A more rational approach is hereby presented, one in which parameter identification (AAR expansion properties) is the result of a formal minimization procedure.

LITERATURE SURVEY

AAR was first identified by Stanton (1940) as a cause for concrete deterioration. However, there were few initial related papers. Probably triggered by an ever-increasing manifestation of the reaction in major structures, there has been recently numerous investigations on AAR. In the context of the presented work, only few related works will be examined. More information can be found in Saouma and Xi (2004).

One of the most extensive and rigorous investigation of AAR has been conducted by Larive (1998) who tested more than 600 specimens with various mixtures and ambient and mechanical conditions. Not only did the author conduct this extensive experimental investigation, but a numerical model has also been proposed for the time expansion of the concrete. In particular, a thermodynamically based model for the expansion evolution was developed, and was then calibrated with the experimental data (Fig. 1).

$$\xi(t,\theta) = \frac{1 - e^{-\frac{t}{\tau_C(\theta)}}}{1 + e^{-\frac{t - \tau_L(\theta, I_\sigma, f_c')}{\tau_C(\theta)}}} \qquad (3)$$

ACI Materials Journal, V. 103, No. 3, May-June 2006.
MS No. 04-411 received July 11, 2005, and reviewed under Institute publication policies. Pertinent discussion including authors' closure, if any, will be published in the March-April 2007 *ACI Materials Journal* if the discussion is received by December 1, 2006.

Victor Saouma *is a Professor of Civil Engineering at the University of Colorado, Boulder, Colo., and is Director of the NEES-NSF Fast Hybrid Testing Laboratory. His research interests include dam engineering, earthquake engineering, concrete deterioration modeling, and fracture mechanics.*

Luigi Perotti *is a PhD Candidate at the California Institute of Technology, Pasadena, Calif. He received his MS from the Department of Structural Engineering of the Technical Institute of Milan. His research interests include theoretical and computational mechanics.*

where τ_L and τ_C are the latency and characteristic times, respectively. The first corresponds to the inflexion point, and the second is defined in terms of the intersection of the tangent at τ_L with the asymptotic unit value of ξ. In a subsequent work, Ulmet al. (2000) have shown the thermal dependency of those two coefficients

$$\begin{cases} \tau_C(\theta) = \tau_C(\theta_0)\exp\left[U_C\left(\frac{1}{\theta} - \frac{1}{\theta_0}\right)\right] \\ \tau_L(\theta, I_\sigma, f'_c) = f(I_\sigma, f'_c)\tau_L(\theta_0)\exp\left[U_L\left(\frac{1}{\theta} - \frac{1}{\theta_0}\right)\right] \end{cases} \quad (4)$$

expressed in terms of the absolute temperature (θ K = 273 + T °C) and the corresponding activation energies. The variables U_L and U_C are the activation energies minimum energy required to trigger the reaction for the latency and characteristic times, respectively, and were determined (for Larive's test) to be

$$U_L = 9400 \pm 500K \quad (5)$$

$$U_C = 5400 \pm 500K \quad (6)$$

To the best of the authors' knowledge, the only other tests for these values were performed by Scrivener (2005) who obtained values within 20% of Larive's values, and the dependency on types of aggregates and alkali content of the cement has not been investigated. Hence, in the absence of other tests, those values can also be reasonably considered as representative of dam concrete. The temperature dependence is highlighted by Fig. 2, where the expansion curve determined in the laboratory at 38 °C is compared with the corresponding one at a dam average temperature of 7 °C.

Beside temperature, other parameters strongly affecting AAR expansion are humidity and confining stresses.

Most recently, Multon (2003) tested AAR expansion under triaxial constraint. Axial traction was applied along one direction of concrete cylinders constrained in the radial directions by steel cylinders. As reported first by Larive (1998) (uniaxial confinement) and later confirmed by Multon et al. (2004) (for triaxial confinement), there is strong evidence of an expansion transfer such that the total volumetric AAR-induced strain is almost constant, irrespective of the confinement. In other words, the expansion is largest in the direction of least resistance. In uniaxially or biaxially loaded cylinders, this results in substantially reduced expansion in the loaded directions and increased expansion in the unconstrained ones. On the other hand, under compressive triaxial confinement, there is nearly equal expansion in all three directions; however, the total volumetric expansion is slightly reduced. Finally, there are strong indications that high compressive hydrostatic stresses retard the reaction.

Accompanying AAR expansion, there is often degradation in tensile strength and elastic modulus (Swamy and Al-Asali 1988). One should exercise some caution, however, as the

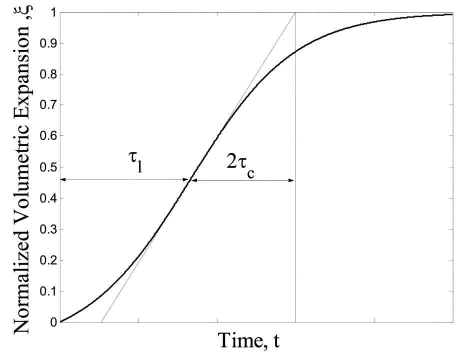

Fig. 1—Normalized expansion curve $(\xi(t) = \varepsilon^{AAR}_{F,Vol}(t)/\varepsilon^{\infty}_{AAR})$.

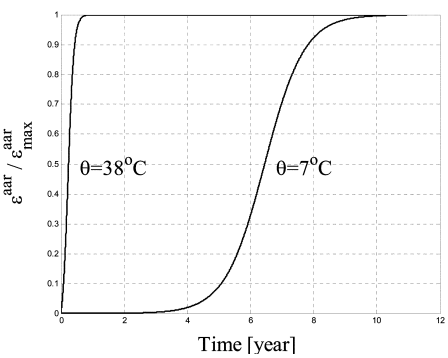

Fig. 2—Effects of temperature on AAR expansion.

degradation observed in laboratory specimens is often much higher than the one recorded in the field.

Whereas a good model for AAR should start with the gel-induced pressure, this is a notoriously complex problem (due to scale) and, in that context, the work of Struble and Diamond (1981a,b) remains most pertinent.

Modeling of AAR expansion has been undertaken by various researchers. Broadly speaking, this modeling falls into one of three categories:

1. Micro models: in which aggregate and cement paste are separately modeled and the transport equation is used to model gel formation through a two-stage process (Suwito et al. 2002; Lemarchand and Dormieux 2000). While essential to properly understand the underlying phenomenon causing AAR, this level of modeling is of little relevance to the structural analysis of AAR-affected structures, as emphasis is on the transport equation for the reactants.

2. Meso models: where emphasis is on the determination of pessimum size effect (Furusawa et al. 1994; Bažant and Steffens 2000).

3. Macro models: where one stays clear from the transport modeling, and emphasis is on a global numerical model for the analysis of a structure. Some of the models fully decouple structural modeling from the reaction kinetics, and others couple those two effects (and some ignore the kinetics all together). One of the earliest models is the one of Charlwood et al. (1992) and Thompson et al. (1994), who identified critical issues related to AAR, namely, the stress dependency—that is, there is no AAR expansion under a compressive stress of approximately 8 MPa, and that the expansion is akin to a thermal one. Subsequently, more refined models have been proposed by Léger et al. (1996) and Huang and Pietruszczak (1999), which focus on the kinetics of the reaction, albeit through empirical models.

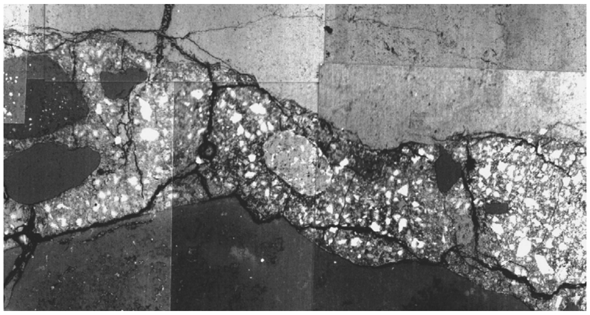

Fig. 3—Stress-induced cracks with potential gel absorption (Scrivener 2003).

Models that address both the kinetics and the mechanical model of AAR have been proposed by Bournazel and Moranville (1997), Capra and Bournazel (1998), Capra and Sellier (2003), Ulm et al. (2000) and Li and Coussy (2002). It is worth noting that the kinetics model (built into a coupled thermo-chemo-mechanical one) of Ulm et al. (2000) (based on the work of Larive [1998]) departs from other empirical models and is probably the most scientifically correct one. It is the one adopted in this work. Bangert and Meschken (2004) recently proposed a coupled model applied to reinforced concrete, and finally, Farage et al. (2004) seem to have finally bridged the gap between scientific rigor and practical applicability to real structures.

Numerous dams worldwide have suffered from AAR, in particular, as reported by Wagner and Newell (1995) (Fontana Dam, U.S.), Gilks and Curtis (2003) (Mactaquac Dam, Canada), Shayan et al. (2000) (Canning Dam, Australia), Peyras et al. (2003) (Chambon dam, France), Jabarooti and Golabtoonchi (2003) (Iran), and Bon et al. (2001) (Pian Telessio Dam, Italy), Portugese National Committee on Large Dams (2003) (Pracana Dam, Portugal), and Malla and Wieland (1999) (a Swiss dam). A comprehensive list of dams suffering from AAR can be found in Acres (2004).

It is worth noting that, in general, dams built in a (relatively) hot climate appear to suffer from AAR at an earlier age than those built at high altitudes and in colder temperatures. Furthermore, when dam rehabilitation did occur, it included one or more of the following: cutting (to relieve the compressive stresses, though accelerating the expansion rate), post-tensioning, or placing an impermeable membrane (whose benefits are not yet well proven).

MODEL

Two different aspects of mathematical modeling of ASR in concrete may be distinguished: 1) the kinetics of the chemical reactions and diffusion processes involved, and 2) the mechanics of fracture that affects volume expansion and causes loss of strength, with possible disintegration of the material (Bažant et al. 2000).

The proposed model (Saouma and Perotti 2004c) is driven by the following considerations:

1. AAR is a volumetric expansion and, as such, cannot be addressed individually along a principal direction without due regard to what may occur along the other two orthogonal ones;
2. Kinetics component is taken from the work of Larive (1998) and Ulm et al. (2000);
3. AAR is sufficiently influenced by temperature to account for its temporal variation in an analysis;
4. AAR expansion is constrained by compression, and is redirected in other less-constrained principal directions. This will be accomplished by assigning weights to each of the three principal directions;
5. Relatively high compressive or tensile stresses inhibit AAR expansion due to the formation of microcracks or macrocracks that absorb the expanding gel;
6. High compressive hydrostatic stresses slow down the reaction;
7. Triaxial compressive state of stress reduces but does not eliminate expansion; and
8. Accompanying AAR expansion is a reduction in tensile strength and elastic modulus.

Hence, the general (uncoupled) equation for the incremental free volumetric AAR strain is given by

$$\dot{\varepsilon}_{vol}^{AAR}(t) = \Gamma_t(f'_t, \sigma_1|\mathrm{COD})\Gamma_c(\bar{\sigma}, f'_c)f(h)\dot{\xi}(t, \theta)\varepsilon^{\infty}\big|_{\theta = \theta_0} \quad (7)$$

where COD is the crack opening displacement; $\xi(t, \theta)$ is a sigmoid curve expressing the volumetric expansion in time as a function of temperature and is given by Eq. (3); ε^{∞} is the laboratory-determined (or predicted) maximum free volumetric expansion at the reference temperature θ_0 (Fig. 1).

The retardation effect of the hydrostatic compressive stress manifests itself through τ_L. Hence, Eq. (4) is expanded as follows

$$\tau_L(\theta, I_\sigma, f'_c) = f(I_\sigma, f'_c)\tau_L(\theta_0)\exp\left[U_L\left(\frac{1}{\theta} - \frac{1}{\theta_0}\right)\right] \quad (8)$$

where

$$f(I_\sigma, f'_c) = \begin{cases} 1 & \text{if } I_\sigma > 0 \\ 1 + \alpha\dfrac{I_\sigma}{3f'_c} & \text{if } I_\sigma \le 0 \end{cases} ;\quad I_\sigma = \sigma_I + \sigma_{II} + \sigma_{III} \quad (9)$$

and I_σ is the first invariant of the stress tensor, and f'_c is the compressive strength. Based on a careful analysis of Multon (2003), it was determined that $\alpha = 4/3$. It should be noted that the stress dependency (through I_σ) of the kinetic parameter τ_L makes the model a truly coupled one between the chemical and mechanical phases. Coupling with the thermal component is a loose one (hence a thermal analysis can be separately run), $0 < g(h) \le 1$ is a reduction function to account for humidity given by

$$g(h) = h^m \quad (10)$$

where h is the relative humidity (Capra and Bournazel 1998). However, one can reasonably assume that (contrary to bridges) inside a dam, $g(h) = 1$ for all temperatures.

$\Gamma_t(f_t|w_c, \sigma_1|\mathrm{COD}_{max})$ accounts for AAR reduction due to tensile cracking (in which case gel is absorbed by macro-cracks) (Fig. 3). A hyperbolic decay with a non-zero residual value is adopted (Fig. 4)

$$\Gamma_t = \begin{cases} \text{Linear elastic} \begin{cases} 1 & \text{if } (\sigma_I \le \gamma_t f'_t) \\ \Gamma_r + (1 - \Gamma_r)\dfrac{\gamma_t f_t^{fictitious}}{\sigma_I} & \text{if } \gamma_t f'_t < \sigma_I \end{cases} \\ \text{Smeared crack} \begin{cases} 1 & \text{if } \mathrm{COD}_{max} \le \gamma_t w_c \\ \Gamma_r + (1 - \Gamma)_r\dfrac{\gamma_t w_c}{\mathrm{COD}_{max}} & \text{if } \gamma_t w_c < \mathrm{COD}_{max} \end{cases} \end{cases} \quad (11)$$

where γ_t is the fraction of the tensile strength beyond which gel is absorbed by the crack, and Γ_r is a residual AAR retention factor for AAR under tension. If an elastic model is used, then f_t is the tensile strength, σ_I is the maximum principal tensile stress. On the other hand, if a smeared crack model is adopted, then COD_{max} is the maximum crack opening displacement at the current Gauss point, and w_c is the maximum crack opening displacement in the tensile softening curve (Wittman et al. 1988). Concrete pores being seldom interconnected, and the gel viscosity relatively high, gel absorption by the pores is not explicitly accounted for. Furthermore, gel absorption by the pores is accounted for by the kinetic equation through the latency time, which depends on concrete porosity. The higher the porosity, the larger the latency time is.

In turn, Γ_c accounts for the reduction in AAR volumetric expansion under compressive stresses (in which case gel is absorbed by diffused microcracks) (Multon 2003)

$$\Gamma_c = \begin{cases} 1 & \text{if } \bar{\sigma} \le 0 \text{ tension} \\ 1 - \dfrac{e^{\beta}\bar{\sigma}}{1 + (e^{\beta} - 1)\bar{\sigma}} & \text{if } \bar{\sigma} > 0 \text{ compression} \end{cases} \tag{12}$$

$$\bar{\sigma} = \frac{\sigma_I + \sigma_{II} + \sigma_{III}}{3f'_c} \tag{13}$$

whereas this expression will also reduce expansion under uniaxial or biaxial confinement (Fig. 4), these conditions are more directly accounted for, as follows, through the assignment of weights.

The third major premise of the model is that the volumetric AAR strain must be redistributed to the three principal directions according to their relative propensity for expansion on the basis of a weight, which is a function of the respective stresses. Whereas the determination of the weight is relatively straightforward for triaxial AAR expansion under uniaxial confinement (for which some experimental data is available), it is more problematic for biaxially or triaxially confined concrete.

Given the principal stress vector defined by σ_k, σ_l, and σ_m, weight to each of those three principal directions needs to be assigned. These weights will control AAR volumetric expansion distribution. For instance, with reference to Fig. 5, three scenarios are considered.

Uniaxial state of stress—where the following three cases are distinguished:

1. In the first case, we have uniaxial tension, and hence, the volumetric AAR strain is equally redistributed in all three directions;

2. Under a compressive stress greater than the limiting on (σ_u), the weight in the corresponding (k) direction should be less than 1/3. The remaining AAR has to be equally redistributed in the other two directions; and

3. If the compressive stress is lower than σ_u, then AAR expansion in the corresponding direction is prevented (weight equal to zero), and thus the other two weights must be equal to 1/2.

Biaxial state of stress—where there is a compressive stress equal to σ_u in one of the three principal directions. In this case, the corresponding weight will always be equal to zero. As to the possible three combinations:

1. Tension in one direction, equal weights of 1/2;

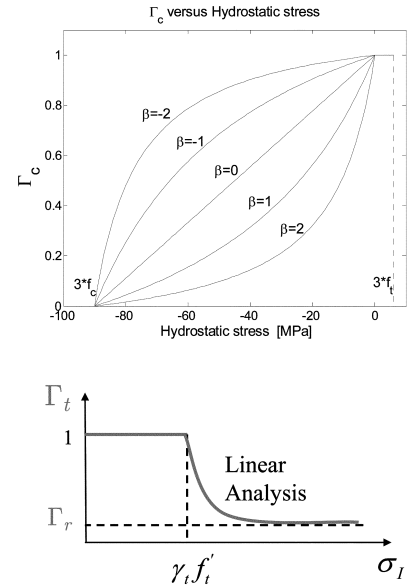

Fig. 4—Graphical representation of Γ_c and Γ_t.

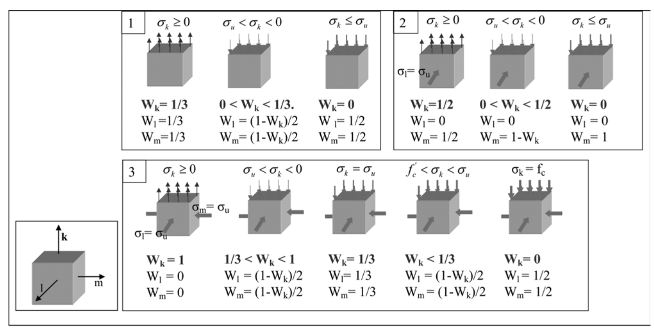

Fig. 5—Weight of volumetric AAR redistribution in selected cases.

2. Compression greater than σ_u in one direction, then the corresponding weight must be less than 1/2, and the remaining weight is assigned to the third direction; and

3. Compression less to σ_u, then the corresponding weight is again zero, and a unit weight is assigned to the third direction.

Triaxial state of stress—in which σ_u acts on two of the three principle directions. The following five cases are identified:

1. Tension along direction k, then all the expansion is along k;

2. Compressive stress greater than σ_u, then we have a triaxial state of compressive stress, and the corresponding weight will be between 1 and 1/3. The remaining complement of the weight is equally distributed in the other two directions;

3. Compression equal to σ_u, hence we have a perfect triaxial state of compressive stress. In this case, there are equal weights of 1/3. It should be noted that the overall expansion is reduced through Γ_c;

4. Compression less than σ_u but greater than the compressive strength. In this case, the weight along k should be less than 1/3, and the remaining equally distributed along the other two directions; and

5. Compression equal to the compressive strength. In this case, the corresponding weight is reduced to zero, and the other two weights are equal to 1/2 each.

Based on the preceding discussion, we generalize this weight allocation scheme along direction k as follows:

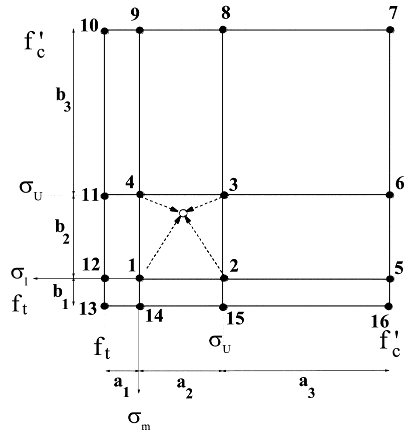

Fig. 6—Weight regions.

1. Given σ_k, identify the quadrant encompassing σ_l and σ_m (Fig. 6).* Weight will be determined through a bilinear interpolation for those four neighboring nodes;
2. Determine the weights of the neighboring nodes from Table 1 through proper linear interpolation of σ_k.
3. Compute the weight from

$$W_k(\sigma_k, \sigma_l, \sigma_m) = \Sigma_{i=1}^{4} N_i(\sigma_l, \sigma_m) W_i(\sigma_k) \tag{14}$$

where N_i is the usual two bilinear shape function used in finite element and is given by

$$N(\sigma_l \sigma_m) = \frac{1}{ab}\lfloor (a-\sigma_l)(b-\sigma_m)\sigma_l(b-\sigma_m)\sigma_l\sigma_m(a-\sigma_l)\sigma_m \rfloor \tag{15}$$

$$W(k) = \lfloor W_1(k) \;\; W_2(k) \;\; W_3(k) \;\; W_4(k) \rfloor^T \tag{16}$$

$$a = (a_1|a_2|a_3) \quad b = (b_1|b_2|b_3) \tag{17}$$

$$\sigma_l = (\sigma_l|f'_c - \sigma_l) \quad \sigma_m = (\sigma_m|f'_c - \sigma_m) \tag{18}$$

The *i-j* stress space is decomposed into nine distinct regions (Fig. 6), where σ_u is the upper (signed) compressive stress below which no AAR expansion can occur along the corresponding direction (except in triaxially loaded cases). Hence, a and b are the dimensions of the quadrant inside which σ_i and σ_j reside.

Weights of the individual nodes are in turn interpolated according to the principal stress component in the third direction σ_k (Table 1). It should be noted that those weights are for the most part based on the work of Larive (1998) and Multon (2003); but in some cases, due to lack of sufficient experimental data, they are based on simple "engineering common sense." A simple example for the evaluation of the weight is shown in the Appendix.

Based on the earlier work of Struble and Diamond (1981a), in which it was reported that no gel expansion can occur at pressures above 11 MPa (though for a synthetic gel), σ_u is taken as –10 MPa. This value was also confirmed by Larive (1998). The concrete tensile and compressive strengths are f_t and f_c, respectively.

*Because compressive stresses are quite low compared with compressive strength, the strength gained through the biaxiality or triaxiality of the stress tensor is ignored (Kupfer and Gerstle 1973). Furthermore, the strength gain is only approximately 14% for equibiaxial compressive stresses (CEB 1983).

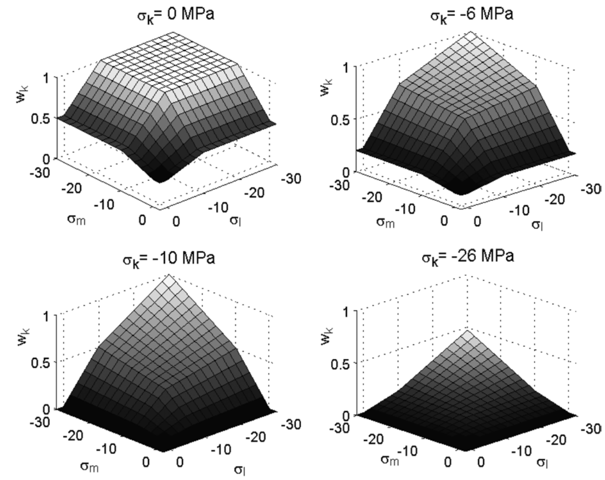

Fig. 7—Relative weights.

Table 1—Triaxial weights

			Weight direction k		
Point	σ_l	σ_m	$\sigma_k \geq 0$	$\sigma_k = \sigma_u$	$\sigma_k = f'_c$
1	0	0	1/3	0	0
2	σ_u	0	1/2	0	0
3	σ_u	σ_u	1	1/3	0
4	0	σ_u	1/2	0	0
5	f_c	0	1/2	0	0
6	f_c	σ_u	1	1/2	0
7	f_c	f_c	1	1	1/3
8	σ_u	f_c	1	1/2	0
9	0	f_c	1/2	0	0
10	f_t	f_c	1/2	0	0
11	f_t	σ_u	1/2	0	0
12	f_t	0	1/3	0	0
13	f_t	f_t	1/3	0	0
14	0	f_t	1/3	0	0
15	σ_u	f_t	1/2	0	0
16	f_c	f_t	1/2	0	0

Individual strain is given by

$$\dot{\varepsilon}_i = W_i \dot{\varepsilon}_V^{AAR} \tag{19}$$

and the resulting relative weights are shown in Fig. 7.

It should be noted that the proposed model will indeed result in an anisotropic AAR expansion. While not explicitly expressed in tensorial form, the anisotropy stems from the different weights assigned to each of the three principal directions. This deterioration being time-dependent, the following time-dependent nonlinear model is considered (Fig. 8)

$$E(t, \theta) = E_0[1 - (1 - \beta_E)\xi(t, \theta)] \tag{20}$$

$$f_t(t, \theta) = f_{t,0}[1 - (1 - \beta_f)\xi(t, \theta)] \tag{21}$$

where E_0 and $f_{t,0}$ are the original elastic modulus and tensile strength, respectively; and β_E and β_f are the corresponding residual fractional values when ε_{AAR} tends to $\varepsilon_{AAR}^{\infty}$.

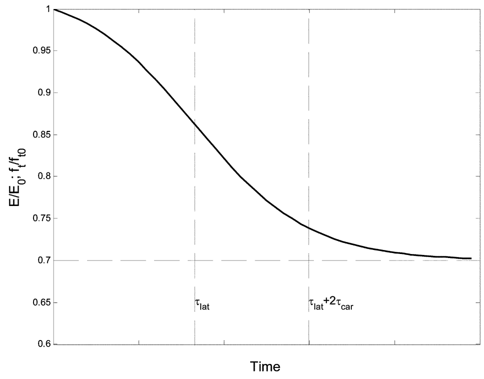

Fig. 8—Degradation of E *and* f'_c.

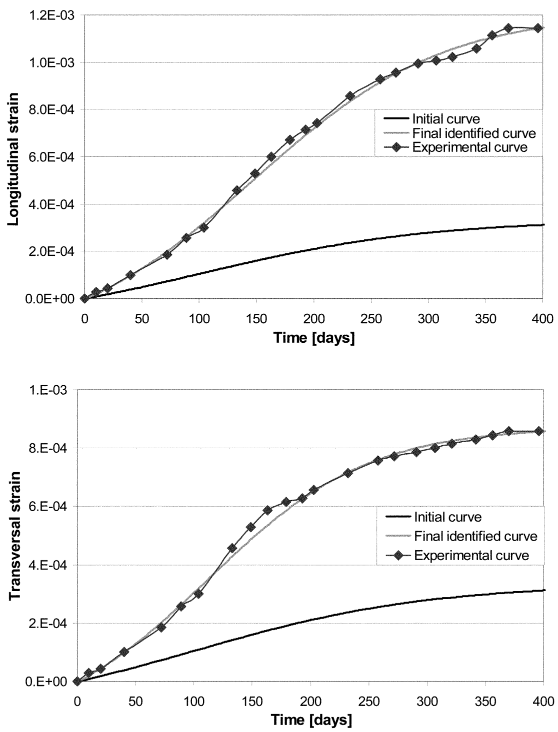

Fig. 9—Multon's test parameter identification results for free expansion; longitudinal and corresponding transversal strains. Initial curve corresponds to initial guess in system identification.

Finally, the possible decrease in compressive strength with AAR was ignored. Most of the literature regarding the mechanical properties of concrete subjected to AAR show little evidence of a decrease in compressive strength (as one would expect because the stresses will be essentially closing the AAR-induced cracks). Furthermore, in dams (gravity and arch), compressive stresses are well below the compressive strength, which is quite different from the tensile stresses.

VALIDATION

Validation and parameter identification was accomplished by analyzing tests of Multon (2003). In those tests, 130 x 240 mm concrete was cast inside a steel cylinder with 3 or 5 mm thickness and subjected to 0, 10, or 20 MPa compressive stresses.

Figure 9 shows the three-dimensional finite element mesh adopted (in addition to an axisymmetric one) along with the results of the parameter identification study under free expansion for τ_l, τ_c, and ε^{∞}. The starting and final parameters are also shown in Table 2. Having determined this initial set of kinetic parameters, another parameter identification for the parameter β in Eq. (12) for the constrained specimens yielded a value of 0.5 (Fig. 10). Finally, the parameter β was used in the subsequent dam analysis. Other kinetic parameters were determined through laboratory experiments of concrete specimens recovered from the dam.

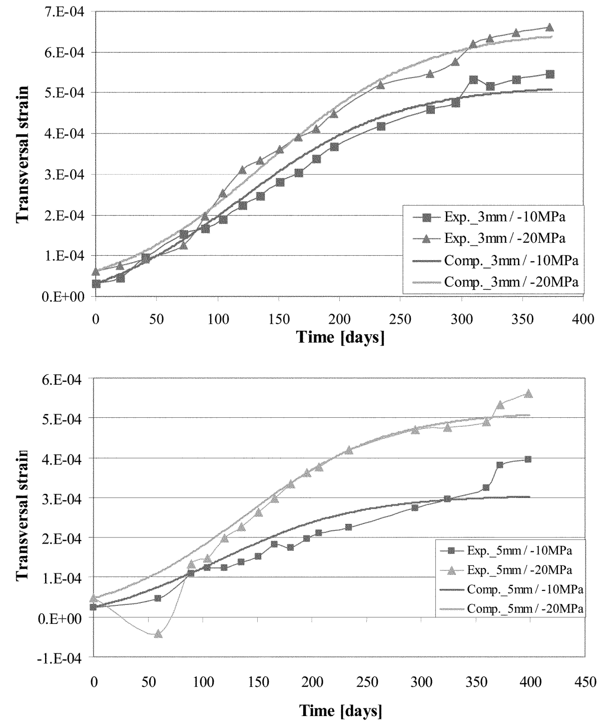

Fig. 10—Comparison between experimental results of Multon and numerical calculations (after parameter identification).

Table 2—System identification for Multon's tests

	Time, days			
	Characteristic	Latency	ε^{∞}	Iterations
Longitudinal expansion				
Initial	100.0	100.0	0.001	—
Final	82.9	146.5	0.00363	8
Transversal expansion				
Initial	100.0	100.0	0.001	—
Final	68.9	111.0	0.00262	7

APPLICATION

Dam analysis data preparation

Finally, a typical application to a two-dimensional analysis of an arch gravity dam is presented. The model has been used in the three-dimensional nonlinear predictive analysis of an actual arch gravity dam, and it was shown that 50 years after dam construction, the reaction will be exhausted (Saouma and Perotti 2004b).

The comprehensive incremental AAR analysis of a concrete dam is relatively complex, irrespective of the selected AAR model, as data preparation for the load can be cumbersome.

First, the seasonal pool elevation variation (for both thermal and stress analysis), and the stress free temperature T_{ref} (typically either the grouting temperature or the average yearly temperature) must be identified, along with the external temperature (Fig. 11).

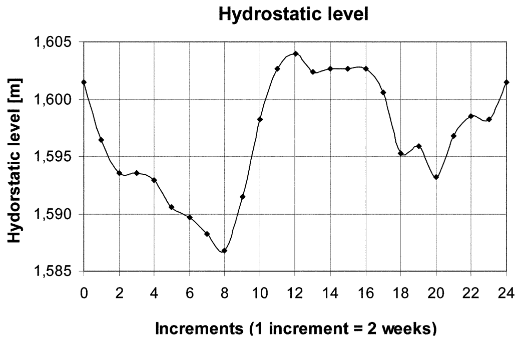

(a) Pool elevation

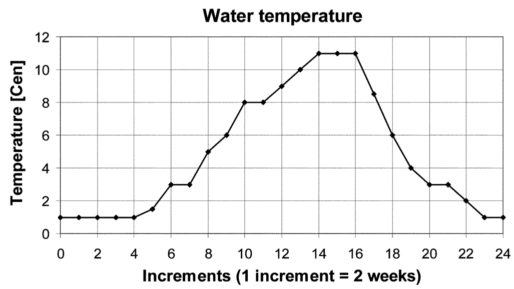

(b) Water temperature

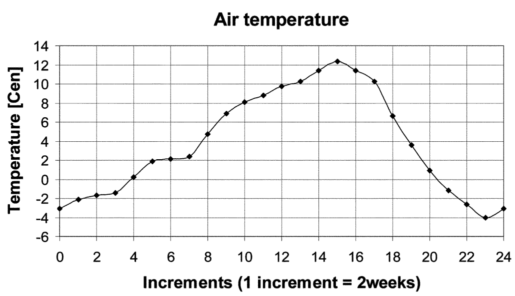

(c) Air temperature

Fig. 11—Yearly variation of hydrostatic and thermal load.

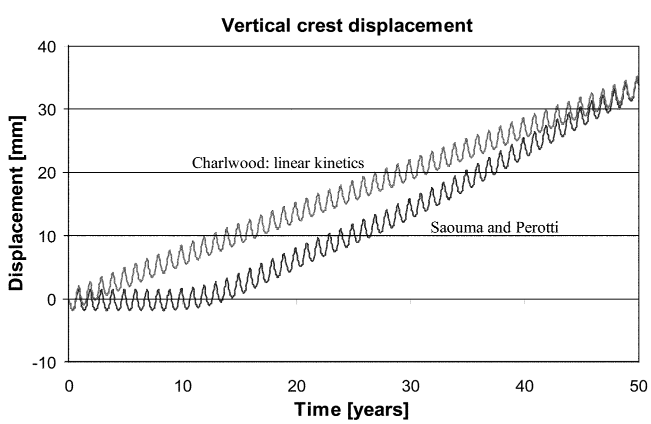

Fig. 12—Yearly variation of vertical crest displacement: upper curve based on Charlwood's model and lower curve based on proposed model.

Then, a transient thermal analysis is performed because the reaction is thermodynamically activated, and the total temperature is hence part of the constitutive model. Heat transfer by conduction only is accounted for. Convection and

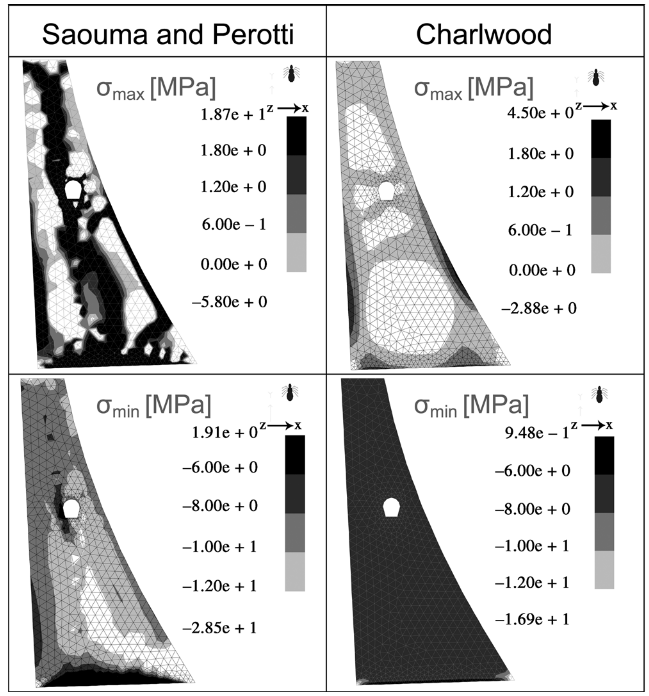

Fig. 13—Principal stress field comparison between proposed and state of practice model (without joints).

radiation are approximated through an additional temperature (Malla and Wieland 1999).

The selected incremental time was 2 weeks, and the initial reference temperature set to zero. Given the external air temperature, the pool elevation and the water temperature boundary conditions were set to this initial boundary value problem. Analysis was performed with Merlin and temperature fields were examined. It was determined that, after 4 years, the temperature field was harmonic with a 1-year frequency. At that point, the analysis was interrupted and $T_{thermal}(x, y, t)$ saved.

Following the thermal analysis, $T_{thermal}(x, y, t)$ must be transferred to $T_{stress}(x, y, t)$ as, in general, we do not have the same finite element mesh (foundations, joints, and cracks are typically not modeled in the thermal analysis). Following this, a comprehensive input data file must be prepared for the stress analysis. It includes:

1. Gravity load (first increment only);
2. $\Delta \cdot T(x, y, t) = \cdot T_{stress}(x, y, t) - T_{ref}$ in an incremental format. This is a delicate step that cannot be overlooked. In particular, the stress analysis is based on the difference between actual and stress-free temperature. In addition, an incremental analysis requires this set of data to be given in an incremental form;
3. Stress-free referenced temperature, which will be added to the temperature data to determine the total absolute temperature needed for AAR;
4. Cantilever and dam/foundation joint characteristics. The first must be accounted for in an arch dam, as the expansion may lead to upstream joint opening. The second must be accounted for as the AAR-induced swelling may result in separation of the dam from the foundation in the central portion of the foundation;
5. Uplift load characteristics (typically in accordance with the upstream hydrostatic load); and
6. AAR data as described as follows. It should be noted that a first-order approximation of the AAR kinetics parameters

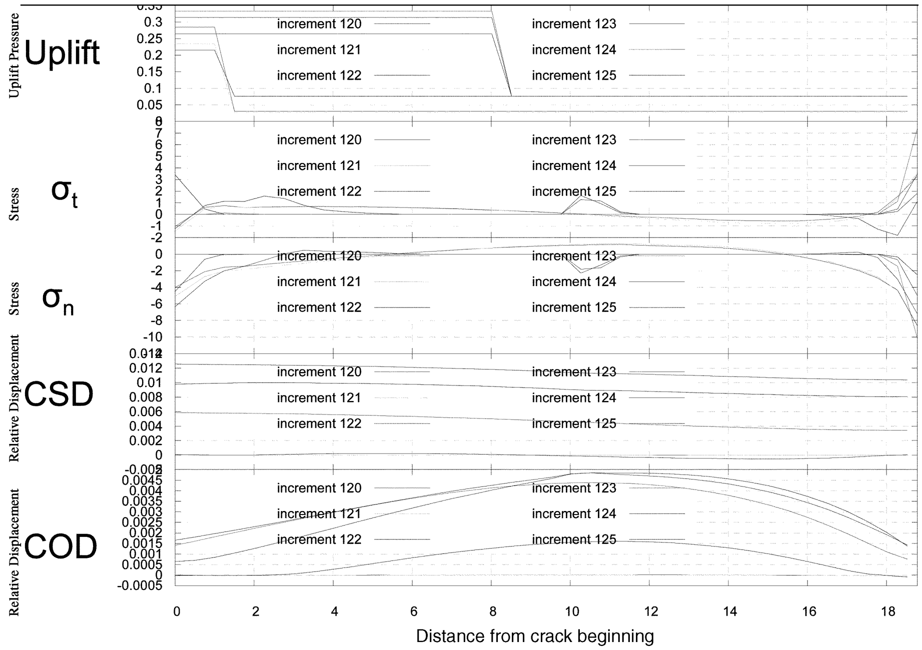

Fig. 14—Dam/foundation interface joint characteristics; uplift, tangential and normal stresses, and cracking and opening displacements along joint.

may be recovered from laboratory tests of dam cores or through an inverse analysis of the dam crest displacement.

Finally, the assembled set of data must be looped over at least 50 years to provide a complete and correct set of natural and essential boundary conditions. For a two-dimensional problem, this will result in files approximately 45 MB.

Dam analysis results

For this preliminary plane strain analysis, a two-dimensional central section of an arch gravity dam is selected. Results based on the proposed model will be contrasted with those obtained using current state of the practice model (Charlwood et al. 1992) with a linear kinetics expansion. In this analysis, creep is not accounted for, and the laboratory-determined Young's modulus is retained throughout both analyses (whereas Charlwood tends to substantially reduce *E* to account for the creep, which in turn may yield potentially lower stresses).

To compare both analyses, final volumetric expansion has been calibrated to yield identical vertical crest displacement after 50 years (Fig. 12), where the proposed model nonlinearity in the crest displacement is caused by the kinetics model and its latency time in particular.

Despite equal final crest displacements, internal field stresses are drastically different as those determined from Charlwood's model are substantially lower than those predicted by the proposed model (Fig. 13). It should be noted that the large discrepancy in stresses is partially caused by the plane strain (which inhibits redistribution in the third direction) assumption of the authors' model. Undoubtedly the lack of stress redistribution in Charlwood's model, however, will lead to an underestimation of the stress field.

Furthermore, due to the influence of the thermal load, the proposed model causes tensile stresses inside the concrete dam, and a lift off along the central portion of the dam-foundation interface (Fig. 14). These internal tensile stresses can possibly explain the formation of the crack observed inside the gallery in the analyzed dam. More details can be found in Saouma and Perotti (2004a).

Finally, no attempt is made to correlate computed crest displacements with the (available) field measurements. The two-dimensional plane strain analysis conducted precludes such a realistic comparison, which is described in a separate, yet-to-be published, study. Furthermore, it should be noted that any model, irrespective of its scientific merits, can be calibrated with field measurements. Only those models solidly based on the chemistry, physics, and mechanics of AAR, however, are likely to yield realistic stress field, which is what ultimately concerns engineers.

CONCLUSIONS

New constitutive model for AAR expansion

This thermo-chemo-mechanical model is rooted in the chemistry (kinetic of the reaction), physics (crack gel absorption, effect of compression), and mechanics of concrete. The major premises of the model is the assumption of a volumetric expansion, redistribution on the basis of weights related to the stress tensor, and contrary to previous models, the stress field affects reaction kinetics, which is a slight modification of the Larive (1998) model.

The model has been used in conjunction with a formal parameter identification paradigm to analyze the three dimensional tests of Multon (2003). A detailed two-dimensional analysis of an arch gravity dam is presented.

ACKNOWLEDGMENTS

The development of the proposed model was made possible through the financial support of the Swiss federal office for water and geology (FOWG). Comments and reviews provided by G. Darbre were particularly constructive. Furthermore, the first author would like to acknowledge the support of the Italian Ministry for University and Research (MIUR), which enabled his visit to the Politecnico di Milano.

REFERENCES

Acres, 2004, http://www.acres.com/AcresGroup/Services/ServHydroASR/indprj.htm.

Bangert, F. D. K., and Meschken, G., 2004, Chemo-Hygro-Mechanical Modeling and Numerical Simulation of Concrete Deterioration Caused by Alkali Silica Reaction, *International Journal of Numerical Analytical Methods and Geomechanics*, V. 28, pp. 689-714.

Bažant, Z. P., and Steffens, A., 2000, "Mathematical Model for Kinetics of Alkali-Silica Reaction in Concrete," *Cement and Concrete Research*, V. 30, pp. 419-428.

Bažant, Z. P.; Zi, G.; and Meyer, C., 2000, "Fracture Mechanics of AAR in Concretes with Waste Glass Particles of Different Sizes," *Journal of Engineering Mechanics*, ASCE, V. 126, No. 3, pp. 226-232.

Bon, E.; Chille, F.; Masarati, P.; and Massaro, C., 2001, "Analysis of the Effects Induced by Alkali-Aggregate Reaction (AAR) on the Structural Behavior of Pian Telessio Dam," *Sixth International Benchmark Workshop on Numerical Analysis of Dams (Theme A)*, Salzburg, Austria.

Bournazel, J., and Moranville, M., 1997, "Durability of Concrete: The Crossroad between Chemistry and Mechanics," *Cement and Concrete Research*, V. 2, No. 10, pp. 1543-1552.

Capra, B., and Bournazel, J., 1998, "Modeling of Induced Mechanical Effects of Alkali Aggregate Reactions," *Cement and Concrete Research*, V. 28, No. 2, pp. 251-260.

Capra, B., and Sellier, A., 2003, "Orthotropic Modeling of Alkali-Aggregate Reaction in Concrete Structures: Numerical Simulations," *Mechanics of Materials*, V. 35, pp. 817-830.

CEB, 1983, "Concrete Under Multiaxial States of Stress Constitutive Equations for Practical Design," *Technical Report Bulletin d'Information 156*, Comité Euro-International du Béton.

Charlwood, R. G.; Solymar, S. V.; and Curtis, D. D., 1992, "A Review of Alkali Aggregate Reactions in Hydroelectric Plants and Dams," *Proceedings of the International Conference of Alkali-Aggregate Reactions in Hydroelectric Plants and Dams*, Fredericton, Canada, 129 pp.

Farage, M.; Alves, J.; and Fairbairn, E., 2004, "Macroscopic Model of Concrete Subjected to Alkali Aggregate Reaction," *Cement and Concrete Research*, V. 34, pp. 495-505.

Furusawa, Y.; Ohga, H.; and Uomoto, T., 1994, "An Analytical Study Concerning Prediction of Concrete Expansion Due to Alkali-Silica Reaction," *Durability of Concrete*, Proceedings of the Third International Conference, SP-145, V. M. Malhotra, ed., American Concrete Institute, Farmington Hills, Mich., pp. 757-780.

Gilks, P., and Curtis, D., 2003, "Dealing with the Effects of AAR on the Water-Retaining Structures at Mactaquac," *Proceedings of the 21st Congress on Large Dams*, Montreal, Quebec, Canada, pp. 681-703.

Huang, M., and Pietruszczak, S., 1999, "Alkali-Silica Reaction: Modeling of Thermomechanical Effects," *Journal of Engineering Mechanics*, ASCE, V. 125, No. 4, pp. 476-487.

Jabarooti, M., and Golabtoonchi, I., 2003, "Alkali-Aggregate Reactivity in South-East of Iran," *Proceedings of the 21st Congress on Large Dams*, Montreal, Quebec, Canada, pp. 53-62.

Kupfer, B., and Gerstle, K., 1973, "Behavior of Concrete under Biaxial Stresses," *Journal of the Engineering Mechanics Division*, ASCE, V. 99, No. 4, pp. 853-866.

Larive, C., 1998, "Apports Combin'es de l'Experimentation et de la Modélisation à la Comprehension del'Alcali-Réaction et de ses Effets Mécaniques," PhD thesis, Thése de Doctorat, Laboratoire Central des Ponts et Chaussées, Paris.

Léger, P.; Côte, P.; and Tinawi, R., 1996, "Finite Element Analysis of Concrete Swelling due to Alkali-Aggregate Reactions in Dams," *Computers & Structures*, V. 60, No. 4, pp. 601-611.

Lemarchand, E., and Dormieux, L., 2000, "A Micromechanical Approach to the Modeling of Swelling due to Alkali-Silica Reaction," *Proceedings of the 14th Engineering Mechanics Conference*, Austin, Tex.

Li, K., and Coussy, O., 2002, "Concrete ASR Degradation: From Material Modeling to Structure Assessment," *Journal of Concrete Science and Engineering*, V. 4, pp. 35-46.

Malla, S., and Wieland, M., 1999, "Analysis of an Arch-Gravity Dam with a Horizontal Crack," *Computers & Structures*, V. 72, No. 1, pp. 267-278.

Multon, S., 2003, "Evaluation Expérimentale et Théorique des Effets Mécaniques de l'Alcali Réaction sur des Structures Modéles," PhD thesis, Université de Marne la Vallée, France.

Multon, S.; Leclainche, G.; Bourdarot, E.; and Toutlemonde, F., 2004, "Alkali-Silica Reaction in Specimens under Multi-Axial Mechanical Stresses," *Proceedings of CONSEC 4* (Concrete Under Severe Conditions), Seoul, pp. 2004-2011.

Peyras, L.; Royet, P.; and Laleu, V., 2003, "Functional Modeling of Dam Performance Loss: Application to the Alkali-Aggregate Reaction Mechanism—Chambon Dam," *Proceedings of the 21st Congress on Large Dams*, Montreal, Quebec, Canada, pp. 853-872.

Portugese National Committee on Large Dams, 2003, "Ageing Process and Rehabilitation of Pracana Dam," *Proceedings of the 21st Congress on Large Dams*, Montreal, Quebec, Canada, pp. 121-138.

Saouma, V., and Perotti, L., 2004a, "2D AAR Parametric Investigation of a Dam," *Technical Report* No. 4, submitted to the Swiss Federal Agency of Water and Geology, Bienne, Switzerland.

Saouma, V., and Perotti, L., 2004b, "AAR Analysis Procedure in Kumo/Merlin," *Technical Report* No. 3, submitted to the Swiss Federal Agency of Water and Geology, Bienne, Switzerland.

Saouma, V., and Perotti, L., 2004c, "Constitutive Model for Alkali Aggregate Reaction," *Technical Report* No. 2, submitted to the Swiss Federal Agency of Water and Geology, Bienne, Switzerland.

Saouma, V., and Xi, Y., 2004, "State of the Art Survey of Alkali-Aggregate Reactions in Dams," *Technical Report* No. 1, submitted to the Swiss Federal Agency of Water and Geology, Bienne, Switzerland.

Scrivener, 2003, personal communication.

Scrivener, 2005, personal communication.

Shayan, A.; Wark, R.; and Moulds, A., 2000, "Diagnosis of AAR in Canning Dam: Characterization of the Affected Concrete and Rehabilitation of the Structure," *Proceedings of the 11th International Conference on AAR*, Quebec, Canada, pp. 1383-1392.

Stanton, T., 1940, "Expansion of Concrete through Reaction between Cement and Aggregate," *Proceedings of ASCE*, V. 66, pp. 1781-1811.

Struble, L., and Diamond, S., 1981a, "Swelling Properties of Synthetic Alkali Silica Gels," *Journal of the American Ceramic Society*, V. 64, No. 11, pp. 652-655.

Struble, L., and Diamond, S., 1981b, "Unstable Swelling Behavior of Alkali Silica Gels," *Cement and Concrete Research*, V. 11, pp. 611-617.

Suwito, A.; Jin, W.; Xi, Y.; and Meyer, C., 2002, "A Mathematical Model for the Pessimum Effect of ASR in Concrete," *Concrete Science and Engineering*, RILEM, V. 4, pp. 23-34.

Swamy, R., and Al-Asali, M., 1988, "Engineering Properties of Concrete Affected by Alkali- Silica Reaction," *ACI Materials Journal*, V. 85, No. 5, Sept.-Oct., pp. 367-374.

Thompson, G.; Charlwood, R.; Steele, R.; and Curtis, D., 1994, "Mactaquac Generating Station Intake and Spillway Remedial Measures," *Proceedings for the Eighteenth International Congress on Large Dams*, V. 1, Q-68, R.24, Durban, South Africa, pp. 347-368.

Ulm, F.; Coussy, O.; Kefei, L.; and Larive, C., 2000, "Thermo-Chemo-Mechanics of ASR Expansion in Concrete Structures, *Journal of Engineering Mechanics*, V. 126, No. 3, pp. 233-242.

Wagner, C., and Newell, V., 1995, "A Review of the History of AAR at Three of the TVA's Dam," *Proceedings of the Second International Conference on AAR in Hydroelectric Plants and Dams*, Tenn., pp. 57-66.

Wittmann, F.; Rokugo, K.; Brühwiler, E.; Mihashi, H.; and Simonin, P., 1988, "Fracture Energy and Strain Softening of Concrete as Determined by Means of Compact Tension Specimens, *Materials and Structures*, V. 21, pp. 21-32.

APPENDIX

A simple example for weight determination is shown here. Assuming that the principal stresses are given by $\lfloor \sigma_l \; \sigma_m \; \sigma_k \rfloor = \lfloor -5.0 \; -8.0 \; -5.0 \rfloor$ MPa, and that f_c, f_t, and σ_u are equal to –30.0, 2.0, and –10.0 MPa, respectively, one seeks to determine W_k. The stress tensors places us inside the quadrant defined by Nodes 1-2-3-4, whose respective weights are equal to

$$W_1 = \frac{1}{2}\left(\frac{1}{3}\right) = \frac{1}{6};\; W_2 = \frac{1}{2}\left(\frac{1}{2}\right) = \frac{1}{4};\; W_3 = \frac{1}{3} + \frac{1}{2}\left(1.0 - \frac{1}{3}\right) = \frac{2}{3};$$

$$W_4 = \frac{1}{2}\left(\frac{1}{2}\right) = \frac{1}{4};$$

a and b are both equal to –10 MPa, and the shape factors will be

$$N_1 = \frac{1}{100}[(-10+5)(-10+8)] = \frac{1}{10};\; N_2 = \frac{1}{100}[-5(-10+8)] = \frac{1}{10};$$

$$N_3 = \frac{1}{100}[(-5)(-8)] = \frac{4}{10};\; N_4 = \frac{1}{100}[-8(-10+5)] = \frac{4}{10};$$

and finally

$$W_k = \frac{1}{10}\frac{1}{6} + \frac{1}{10}\frac{1}{4} + \frac{4}{10}\frac{2}{3} + \frac{4}{10}\frac{1}{4} = 0.40833 .$$